Biochemical Pharmacology 79 (2010) 1072–1080

Contents lists available at ScienceDirect

Biochemical Pharmacology

journal homepage: www.elsevier.com/locate/biochempharm

Cytosolic NADP$^+$-dependent isocitrate dehydrogenase regulates cadmium-induced apoptosis

Seoung Woo Shin, In Sup Kil, Jeen-Woo Park *

School of Life Sciences and Biotechnology, College of Natural Sciences, Kyungpook National University, Taegu 702-701, Republic of Korea

ARTICLE INFO

Article history:
Received 14 September 2009
Accepted 20 November 2009

Keywords:
Cadmium
Antioxidant enzyme
siRNA
Apoptosis
Redox status

ABSTRACT

Cadmium ions have a high affinity for thiol groups. Therefore, they may disturb many cellular functions. We recently reported that cytosolic NADP$^+$-dependent isocitrate dehydrogenase (IDPc) functions as an antioxidant enzyme to supply NADPH, a major source of reducing equivalents to the cytosol. Cadmium decreased the activity of IDPc both as a purified enzyme and in cultured cells. In the present study, we demonstrate that the knockdown of IDPc expression in HEK293 cells greatly enhances apoptosis induced by cadmium. Transfection of HEK293 cells with an IDPc small interfering RNA significantly decreased the activity of IDPc and enhanced cellular susceptibility to cadmium-induced apoptosis as indicated by the morphological evidence of apoptosis, DNA fragmentation and condensation, cellular redox status, mitochondria redox status and function, and the modulation of apoptotic marker proteins. Taken together, our results suggest that suppressing the expression of IDPc enhances cadmium-induced apoptosis of HEK293 cells by increasing disruption of the cellular redox status.

1. Introduction

Cadmium (Cd^{2+}) is a metal frequently used in various industrial activities and a ubiquitous environmental contaminant present in tobacco smoke and food [1]. This metal is toxic to hepatic, cardiovascular, respiratory, immune and renal systems [2]. It has been demonstrated that cadmium toxicity is associated with increased production of reactive oxygen species (ROS) [3]. Since the potential role of ROS have been proposed as mediators for apoptotic cell death, the involvement of oxidative stress in cadmium-induced apoptosis was suggested [4]. Previous studies have shown that cadmium can induce apoptosis of many tissues *in vivo* and *in vitro* [5]. In addition, cadmium ions have a high affinity to thiol groups and easily form cadmium–thiol complexes [6]. Since thiol groups are usually involved in the function of many enzymes, structure proteins and receptors, the cadmium–thiol complexes possibly disturb many functions of cells [7].

Isocitrate dehydrogenase (ICDH) enzymes catalyze the oxidative decarboxylation of isocitrate to α-ketoglutarate [8]. In mammals, the family of ICDHs is classified on the basis of their cofactor and intracellular localization: cytosolic NADP$^+$-dependent ICDH (IDPc) encoded by *IDH1* gene, mitochondrial NADP$^+$-dependent ICDH (IDPm) encoded by *IDH2* gene, and mitochondrial NAD$^+$-dependent ICDH encoded by *IDH3* gene [9]. In addition to different subcellular localization, two NADP$^+$-dependent isoenzymes exhibit differences in chromosomal loci and gene sequences [10,11], and different tissue-specific expression [12]. IDPc is responsible for production of NADPH in cytoplasm. NADPH is an essential reducing equivalent for the maintenance of antioxidant glutathione in its reduced state and for the activity of NADPH-dependent thioredoxin system, which plays an important role in the antioxidant system [13,14]. It is also required in maintaining the antioxidant catalase in its active form [15].

The present investigation was undertaken to study the inhibitory effect of cadmium on the IDPc activity. In addition, the role of IDPc in cellular defense against cadmium-induced apoptosis was evaluated with HEK293 cells transfected with IDPc small interfering RNA (siRNA). The data indicate that the cadmium-mediated down-regulation of IDPc may result in the perturbation of cellular antioxidant mechanisms and may enhance the cadmium-induced cell apoptosis.

2. Materials and methods

2.1. Materials

Isocitrate, β-NADP$^+$, NADPH, cadmium chloride ($CdCl_2$), GSH, GSSG, dithiothreitol (DTT), xylenol orange, 5,5′-dithiobis(2-nitrobenzoic acid) (DTNB), N-acetylcysteine (NAC), L-buthionine-(*S*,*R*)-sulfoximine (BSO), anti-rabbit IgG fluorescein isothiocyanate (FITC) conjugated secondary antibody, and propidium iodide (PI) were purchased from Sigma Chemical Co. (St. Louis, MO). 7-Amino-4-

* Corresponding author. Tel.: +82 53 950 6352; fax: +82 53 943 2762.
E-mail address: parkjw@knu.ac.kr (J.-W. Park).

0006-2952/$ – see front matter © 2009 Elsevier Inc. All rights reserved.
doi:10.1016/j.bcp.2009.11.014

chloromethylcoumarin (CellTracker™ blue CMAC), 5,5′,6,6′-tetrachloro-1,1′,3,3′-tetraethylbenzimidazole carbocyanine iodide (JC-1), dihydrorhodamine 123, Rhodamine 123, dihydroethidium (DHE), and 2′,7′-dichlorofluorescein diacetate (DCFH-DA) were purchased from Molecular Probes (Eugene, OR). Antibodies were purchased from Santa Cruz (Santa Cruz, CA) and Cell Signaling (Beverly, MA). Ac-Asp-Glu-Val-Asp-pNA (Ac-DEVD-pNA) was obtained from Calbiochem (La Jolla, CA). Recombinant mouse IDPc was prepared as previously described [16]. A purified mouse IDPc was used to prepare polyclonal anti-IDPc antibodies in rabbits.

2.2. Cell culture

HEK293, a human embryonic kidney cell line, were cultured at 37 °C in a humidified atmosphere containing 5% CO_2, in Dulbecco's modified Eagle's medium supplemented with 10% FBS, 2 mM glutamine, and 100 units/ml penicillin/streptomycin.

2.3. Site-directed mutagenesis and preparation of recombinant proteins

Site-directed mutagenesis was performed using the Quik-Change site-directed mutagenesis kit (Stratagene, La Jolla, CA). The following mutagenic primers were used: 5′-GCTTCATCTGGGC-CAGTAAAAACTATG-3′ for C269S and 5′-GGACTTGGCTGCTAGCAT-TAAAGGTTTAC-3′ for C379S, respectively, in which the substituted serine codon is underlined. To prepare recombinant proteins, *E. coli* transformed with pET-22b(+) vector containing the cDNA insert for human IDPc or mutant IDPc (C269S and C379S) constructs was grown and lysed, and His-tagged proteins were purified on nickel-nitrilotriacetic acid agarose as described previously [16].

2.4. Knockdown of IDPc by siRNA

IDPc siRNA and control (scrambled) siRNA were purchased from Samchully Pham (Seoul, Korea). The sequences of the dsRNAs of IDPc and control used in the current experiments are as follows. For IDPc, sense and antisense IDPc siRNA are 5′-GGACUUGGCUGC-UUGCAUUdTdT-3′ and 5′-AAUGCAAGCAGCCAAGUCCdTdT-3′. For scrambled control, sense and antisense siRNAs are 5′-CUGAUGAC-CUGAGUGAAUGdTdT-3′ and 5′-CAUUCACUCAGGUCAUCAGdTdT-3′, respectively. HEK293 cells were transfected with 40 nM oligonucleotide by using Lipofectamine RNAi MAX (Invitrogen) in serum-free conditions according to the manufacturer's protocol. After incubation for 4 h, the cells were washed and supplemented with fresh medium containing 10% FBS.

2.5. Enzyme assays

IDPc (5 μg) or cytosolic fraction of cells was added to 1 ml of 40 mM Tris buffer, pH 7.4 containing $NADP^+$ (2 mM), $MgCl_2$ (2 mM), and isocitrate (5 mM). Activity of IDPc was determined by the production of NADPH at 340 nm at 25 °C. Caspase-3 activity was determined with the colorimetric agent Ac-DEVD-pNA (caspase-3 substrate) as described previously [17]. Grx1 activity was determined as described previously [18].

2.6. Immunocytochemistry

Cells were seeded on 60 mm dishes to a density of 40–60% 1 day before transfection of siRNA. After transfection of scrambled or IDPc siRNA, cells were incubated for 2 days, and then cells were fixed with 4% formaldehyde at room temperature for 20 min. The IDPc level in HEK293 cells was determined with anti-IDPc antibody (1:200 dilution) and anti-human IgG–FITC (excitation, 488 nm; emission, 520 nm) conjugate (1:500 dilution) as a secondary antibody, and then fluorescence was observed using a fluorescence microscope.

2.7. RT-PCR analysis of IDPc

RNA was isolated using the RNeasy kit (Qiagen) according to the manufacturer's instruction. The cDNA template was then amplified by quantitative RT-PCR using the following specific primers: IDPc, 5′-GCT TCA TCT GGG CCA GTA AAA ACT ATG-3′ (forward) and 5′-GTA AAC CTT TAA TGC TAG CAG CCA AGT CC-3′ (reverse); and actin, 5′-TCT ACA ATG AGC TGC GTG TG-3′ (forward) and 5′-ATC TCC TTC TGC ATC CTG TC-3′ (reverse). The amplified DNA products were resolved on a 1% nondenaturing agarose gel, which was stained with ethidium bromide.

2.8. Cellular redox status

NADPH was measured using the enzymatic cycling method as described by Zerez et al. [19] and expressed as the ratio of NADPH to the total NADP pool. Intracellular ROS generation was measured using the oxidant-sensitive fluorescent probe DCFH-DA with fluorescence microscopy. Intracellular peroxide concentrations were also determined using a ferric sensitive dye, xylenol orange, as described [20]. Superoxide anion production was measured using the fluorescent probe DHE with a fluorescence microscope [20]. Intracellular GSH levels were determined by using a GSH-sensitive fluorescence dye CMAC. HEK293 cells (1×10^6 cells/ml) were incubated with 5 μM CMAC cell tracker for 30 min. The images of CMAC cell tracker fluorescence by GSH was analyzed by the Zeiss Axiovert 200 inverted microscope at fluorescence DAPI region (excitation, 351 nm; emission, 380 nm) [21]. The concentration of total glutathione was determined by the rate of formation of 5-thio-2-nitrobenzoic acid at 412 nm ($\varepsilon = 1.36 \times 10^4\ M^{-1}\ cm^{-1}$), and GSSG was measured by the DTNB-GSSG reductase recycling assay after treating GSH with 2-vinylpyridine [22].

2.9. FACS

Apoptotic cells were analyzed by flow cytometry using PI. Labeled nuclei were subjected to flow cytometric analysis and then gated on light scatter to remove debris, and the percentage of nuclei with a sub-G_1 content was considered apoptotic cells.

2.10. DNA fragmentation assay

Oligonucleosomal DNA fragmentation was identified by agarose gel electrophoresis [17]. DNA fragmentation was also determined using the diphenylamine assay [23].

2.11. Mitochondrial redox status and damage

The fluorescent probe JC-1 was used to estimate mitochondrial membrane potential. JC-1 (10 μM) was added to the cells and then incubated at 37 °C for 30 min. The ratio of the intensity of green fluorescent monomers to the intensity of aggregates of JC-1 is directly related to mitochondrial membrane potential [24]. Mitochondrial membrane permeability transition (MPT) was measured by the incorporation of rhodamine 123 dye into the mitochondria, as previously described [20]. Cells were treated with 5 μM rhodamine for 15 min and excited at 488 nm with an argon laser. The levels of mitochondrial hydrogen peroxide were determined with the oxidant-sensitive fluorescent probe DHR 123 with fluorescent microscope [20]. Cells were incubated for 20 min at 37 °C with 5 μM DHR123 and cells loaded with fluorescent probes were imaged with a fluorescence microscope.

2.12. Cellular fractionation

To analyze the subcellular distribution of cytochrome *c* and apoptosis-inducing factor (AIF), cells were fractionated into cytosolic and membrane-bound fractions using low concentrations of digitonin, which selectively permeabilizes the plasma membrane to release the cytosol [25]. Cells were extracted with digitonin in sucrose buffer (250 mM sucrose, 75 mM NaCl, 1 mM NaH_2PO_4, 8 mM $NaHPO_4$, 1 mM PMSF, 5 μg/ml leupeptin, 21 μg/ml aprotinin, 12.5 μg/ml digitonin) to collect the cytosol. Cells were centrifuged at 10,000 × *g* for 5 min, and the supernatants were immunoblotted with antibodies against cytochrome *c* and AIF.

2.13. Western blot analysis

Proteins were resolved on a 10–12.5% SDS-polyacrylamide gel. Following electrophoretic transfer of proteins onto nitrocellulose membranes, the proteins were subsequently hybridized with primary antibody (1:2000 dilution) and followed with a horseradish peroxidase-conjugated second antibody (1:2000 dilution). Finally, the protein bands were visualized using the enhanced chemiluminescence detection kit (Amersham Pharmacia Biotech).

2.14. Quantitation of relative fluorescence

The averages of fluorescence intensity from fluorescence images were calculated as described [26].

2.15. Statistical analysis

The difference between two mean values was analyzed by Student's *t*-test and was considered to be statistically significant when $p < 0.05$.

3. Results

3.1. Inactivation of IDPc by cadmium

Fig. 1A and B shows that cadmium inhibits IDPc activity in a time- and concentration-dependent manner, reaching 60% inhibition at 50 μM after 1 h incubation. One possible mechanism for the inhibition of IDPc by cadmium could be the oxidation of reactive sulfhydryl groups present on IDPc. We tested this hypothesis using thiols such as DTT and GSH. The inhibition of IDPc by cadmium was completely protected by both DTT and GSH (Fig. 1C). To evaluate the protective effect of different substrates on the inhibition of IDPc by cadmium, IDPc was pre-incubated with either $NADP^+$ or isocitrate/$MgCl_2$ for 1 h. Following the removal of excess substrate using a Centricon filter unit (10 kDa cutoff), IDPc samples were treated further with various concentrations of cadmium for 1 h. The addition of isocitrate/$MgCl_2$ completely protected IDPc from inactivation, while $NADP^+$ did not exhibit a protective effect against the cadmium-induced inhibition of IDPc (Fig. 1D). To determine which cysteine residue is a target for cadmium, IDPc wild-type and cysteine mutants were treated with various concentrations of cadmium for 1 h at 37 °C. The remaining activity of the C269S mutant was not significantly

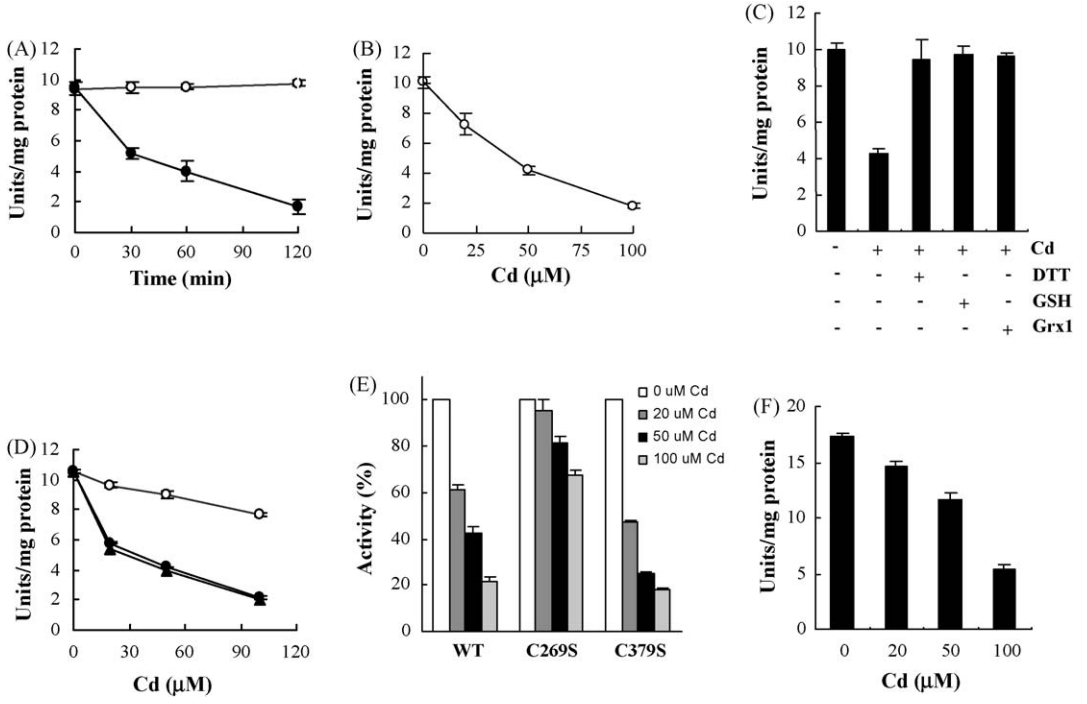

Fig. 1. Inactivation of IDPc by cadmium. (A) Time-dependent inactivation of IDPc by cadmium. IDPc was incubated with 50 μM cadmium (*closed circles*) or without cadmium (*open circles*) at 37 °C and an aliquot of the incubation mixture was taken at indicated times, and then the remaining activity was determined. Data are presented as means ± S.D. of five separate experiments. (B) Concentration-dependent inactivation of IDPc by cadmium. IDPc was incubated with 0–100 μM cadmium at 37 °C for 1 h. The remaining activity was determined. Data are presented as means ± S.D. of five separate experiments. (C) IDPc was incubated with 50 μM cadmium in the absence or in the presence of 2 mM GSH or 10 mM DTT. Data are presented as means ± S.D. of five separate experiments. (D) Effect of substrates on the inactivation of IDPc by cadmium. IDPc was pre-treated with buffer alone (*triangles*), 1 mM $NADP^+$ (*closed circles*) or isocitrate (4 mM)-Mg^{2+} (2 mM) (*open circles*) for 1 h at 37 °C. After excess substrates were removed by a Centricon filter unit IDPc samples were further treated with various concentrations of cadmium for 1 h. Data are presented as means + S.D. of five separate experiments. (E) Identification of target cysteine residue on IDPc. Wild-type and mutant IDPc proteins were treated with various concentrations of cadmium for 1 h at 37 °C, and the remaining activity was determined. Activities are given as a percentage of the control value. Data are presented as means + S.D. of five separate experiments. (F) Inactivation of IDPc in cadmium-treated HEK293 cells. HEK293 cells were incubated with various concentrations of cadmium for 8 h at 37 °C and the activity of IDPc was determined. Data are presented as means + S.D. of five separate experiments.

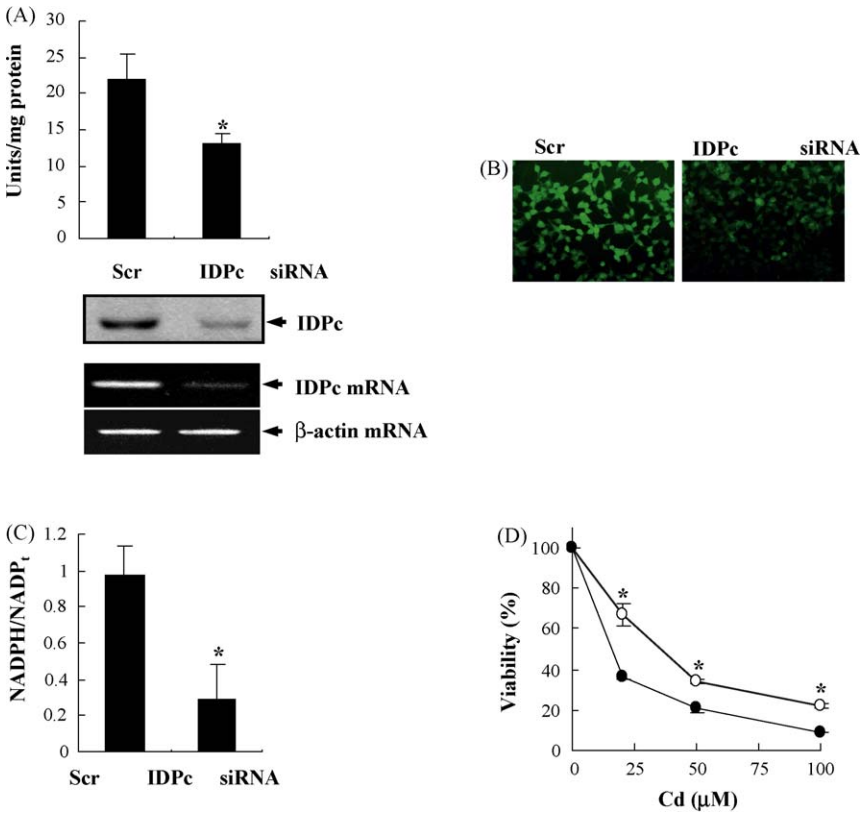

Fig. 2. Knockdown of IDPc by siRNA in HEK293 cells. (A) HEK293 cells were transfected with scrambled siRNA (Scr) or IDPc siRNA. After 48 h, the transfected cells were disrupted by sonication, and then the activity, mRNA levels and protein levels of IDPc were determined. Data are presented as means ± S.D. of three separate experiments. $^*p < 0.01$ versus scrambled siRNA-transfected cells. (B) Immunochemical detection of IDPc in HEK293 cells. The transfected cells were stained with anti-IDPc antibody and anti-human IgG FITC conjugate as a secondary antibody. Fluorescence images were observed under microscopy. (C) NADPH versus total NADP pool in HEK293 transfectant cells. Data are presented as means ± S.D. of three separate experiments. $^*p < 0.01$ versus scrambled siRNA-transfected cells. (D) Viability of transfectant cells exposed to cadmium. After IDPc siRNA- (*closed circles*) or control scrambled siRNA-transfected (*open circles*) HEK293 cells were exposed to various concentrations of cadmium for 24 h at 37 °C, viability of cells was determined by MTT assay. Data are presented as means ± S.D. of three separate experiments. $^*p < 0.01$ versus IDPc siRNA-transfected cells exposed to cadmium.

affected by cadmium, whereas the C378S mutant was inhibited in a manner similar to IDPc wild-type (Fig. 1E). Taken together, we propose that Cys^{269} is a target for the inhibition of IDPc by cadmium. To test whether cellular IDPc was inactivated, HEK293 cells were treated with cadmium (0–100 μM) for 8 h. We found that cell-derived IDPc activity was lost in a dose-dependent manner (Fig. 1F).

3.2. Knockdown of cellular IDPc by siRNA

siRNA methodologies are rapidly being established, with promising results in the inhibition of specific gene expression in mammalian cells [27]. To test whether an *in vitro*-transcribed siRNA specific for the mRNA of human IDPc displayed knockdown activity, we assayed the activity and expression of the IDPc mRNA and protein in HEK293 cells transiently transfected with IDPc siRNA. The siRNA-transfected HEK293 cells exhibited significantly reduced IDPc mRNA and protein expression levels when compared with that of control cells transfected with a scrambled siRNA (Fig. 2A). In addition, we used immunocytochemistry to confirm the specific loss of the IDPc protein upon transfection with the siRNA (Fig. 2B). The ratio for [NADPH]/[$NADP^+$ + NADPH] was significantly decreased in IDPc siRNA-transfected cells compared to control cells (Fig. 2C). When cultured HEK293 cells were treated with various concentrations of cadmium, we observed concentration-dependent loss of cell viability. However, HEK293 cells transfected with the IDPc siRNA were significantly more sensitive to cadmium than control cells transfected with the scrambled siRNA (Fig. 2D).

3.3. Role of IDPc siRNA in apoptosis induced by cadmium

We also evaluated the effects of transfection of the IDPc siRNA on the cellular features of cadmium-induced apoptosis. To observe the morphological characteristics of apoptosis, we exposed HEK293 cells to 20 μM cadmium for 8 h, stained them with Hoechst 33452, and examined them by fluorescence microscopy. Control cells showed an even distribution of the fluorescent stain and round homogenous nuclei. In contrast, the number of apoptotic cells increased in the IDPc siRNA-transfected cells exposed to cadmium and displayed a reduction in cell volume, bright staining and condensed fragmented nuclei (Fig. 3A). To determine the possible involvement of the IDPc siRNA in the regulation of the cell cycle, we analyzed the effect of the IDPc siRNA on HEK293 cells exposed to cadmium by flow cytometry. When HEK293 cells were exposed to 20 μM cadmium for 8 h, the sub-G_1 fraction of the cells increased markedly in IDPc siRNA-transfected cells compared to the control cells. Cadmium-induced apoptosis in HEK293 cells was determined by the measurement of DNA ladder formation using agarose gel electrophoresis. DNA fragmentation was further confirmed by the diphenylamine assay and we found that DNA fragmentation was enhanced in IDPc siRNA-transfected HEK293 cells compared to control cells upon exposure to cadmium (Fig. 3C and D). We also evaluated the effect of the attenuated expression of IDPc on the modulation of apoptotic marker proteins in HEK293 cells. Caspase-3 activation in HEK293 cells was assessed by caspase colorimetric assay and by immunoblot analysis. Caspase-3 activity increased markedly in IDPc siRNA-transfected HEK293 cells compared to control cells upon exposure to

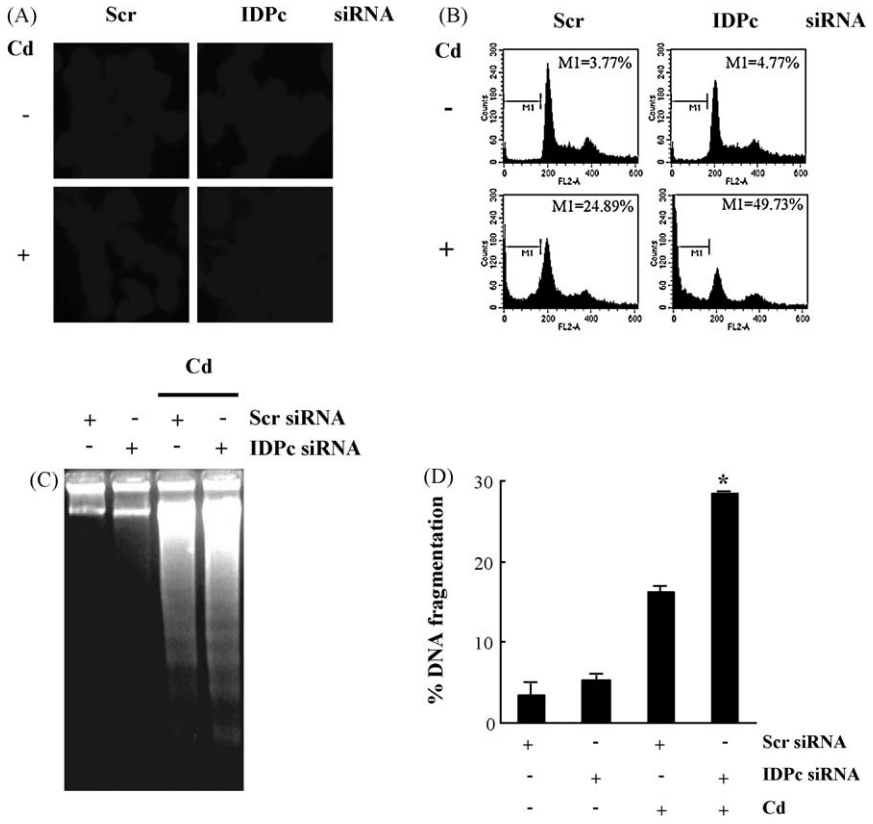

Fig. 3. Cadmium-induced apoptosis in IDPc siRNA transfectant HEK293 cells. (A) HEK293 cells were treated with 20 μM cadmium for 8 h. Cadmium-mediated morphologic changes were examined by Hoechst 33452 staining and observed under fluorescence microscope. (B) Cell cycle analysis with cellular DNA content was examined by flow cytometry. The sub-G_1 region (presented as 'M1') includes cells undergoing apoptosis. The number of each panel refers to the percentage of apoptotic cells. (C) Agarose gel electrophoresis of nuclear DNA fragments of HEK293 transfectant cells exposed to 20 μM cadmium for 8 h. (D) DNA fragmentation was determined using a diphenylamine assay. Data are presented as means ± S.D. of three separate experiments. $^*p < 0.01$ versus scrambled siRNA-transfected cells exposed to cadmium.

cadmium. As shown in Fig. 4A, cleavage of procaspase-3, induced by cadmium, was more pronounced in IDPc siRNA-transfected cells. The cleaved products of PARP and lamin B, which indicate the imminent induction of apoptosis, increased markedly in IDPc siRNA-transfected cells, compared to control cells upon exposure to cadmium (Fig. 4B). Taken together, our results indicate that cadmium induces cleavage of procaspase-3 to the active form of caspase-3, which induces the degradation of PARP and lamin B. Next, we used immunoblot analysis to evaluate the abundance of Bcl-2, an antiapoptotic protein, and of Bax, a proapoptotic protein, in order to determine the role played by the mitochondrial apoptotic pathway in the cadmium-induced apoptosis of HEK293 cells. Upon exposure to cadmium the abundance of Bcl-2 decreased whereas that of Bax increased markedly in IDPc siRNA-transfected cells compared to control cells (Fig. 4B). It has been reported that the expression of stress proteins such as heat shock proteins and metallothionein are induced in response to cadmium exposure [28]. HSP 70 increased higher in IDPc siRNA-transfected cells compared to control cells. As shown in Fig. 4C, the abundance of cytochrome *c*, a proapoptotic protein, and AIF in the cytosol of HEK293 cells was significantly increased in IDPc siRNA-transfected cells, compared to control cells, when exposed to cadmium. The decreased level of cytochrome *c* in the mitochondrial fraction and the increased level of AIF in the nuclear fraction of IDPc siRNA-transfected cells exposed to cadmium were also observed. The activation of JNK has been implicated in the induction of apoptosis, whereas the activation of ERK and Akt has been considered as a sign of cellular survival [29]. To evaluate the effect of IDPc siRNA on the cadmium-mediated signaling pathway, we examined the activation of MAPKs by Western blot analysis. We found that the level of phospho-JNK increased, but the levels of phospho-ERK and phospho-Akt decreased in HEK293 cells transfected with IDPc siRNA to upon exposure to cadmium (Fig. 4D). The time course of ERK activation differed from those observed to control cells and IDPc siRNA-transfected cells. The time course of ERK activation in the presence of cadmium showed a significant increase of pERK after 30 min of treatment in IDPc siRNA-transfected cells whereas ERK activation was observed after 2 h in control cells. At any rate, the level of pERK was lower in IDPc siRNA-transfected cells compared to control cells, when cells were exposed to cadmium for 8 h.

3.4. Role of IDPc siRNA in redox status

We hypothesized that the knockdown of IDPc expression in HEK293 cells would decrease cellular reducing potential and increase ROS formation, which in turn, induce apoptosis. Cellular ROS levels were measured using the fluorescent probe DCFH-DA and DHE. As shown in Fig. 5A and B, there was a greater increase of DCF and DHE fluorescence in IDPc siRNA-transfected cells than in control cells upon exposure to cadmium. We also observed significantly higher intracellular levels of peroxides, as measured by xylenol orange, in IDPc siRNA-transfected HEK293 cells exposed to cadmium, compared to control cells (Fig. 5C). When cellular GSH levels were measured using the GSH-sensitive fluorescent dye CMAC, the CMAC fluorescence in IDPc siRNA-transfected HEK293 cells exposed to cadmium decreased significantly compared to control cells (Fig. 5D). In addition, the ratio of [GSSG]/[GSH_t], which may reflect the efficiency of GSH turnover, was significantly higher in cadmium-exposed HEK293 cells transfected with IDPc siRNA, than in control cells (Fig. 5E). When intracellular GSH was further depleted by BSO, a specific inhibitor of γ-glutamylcysteine

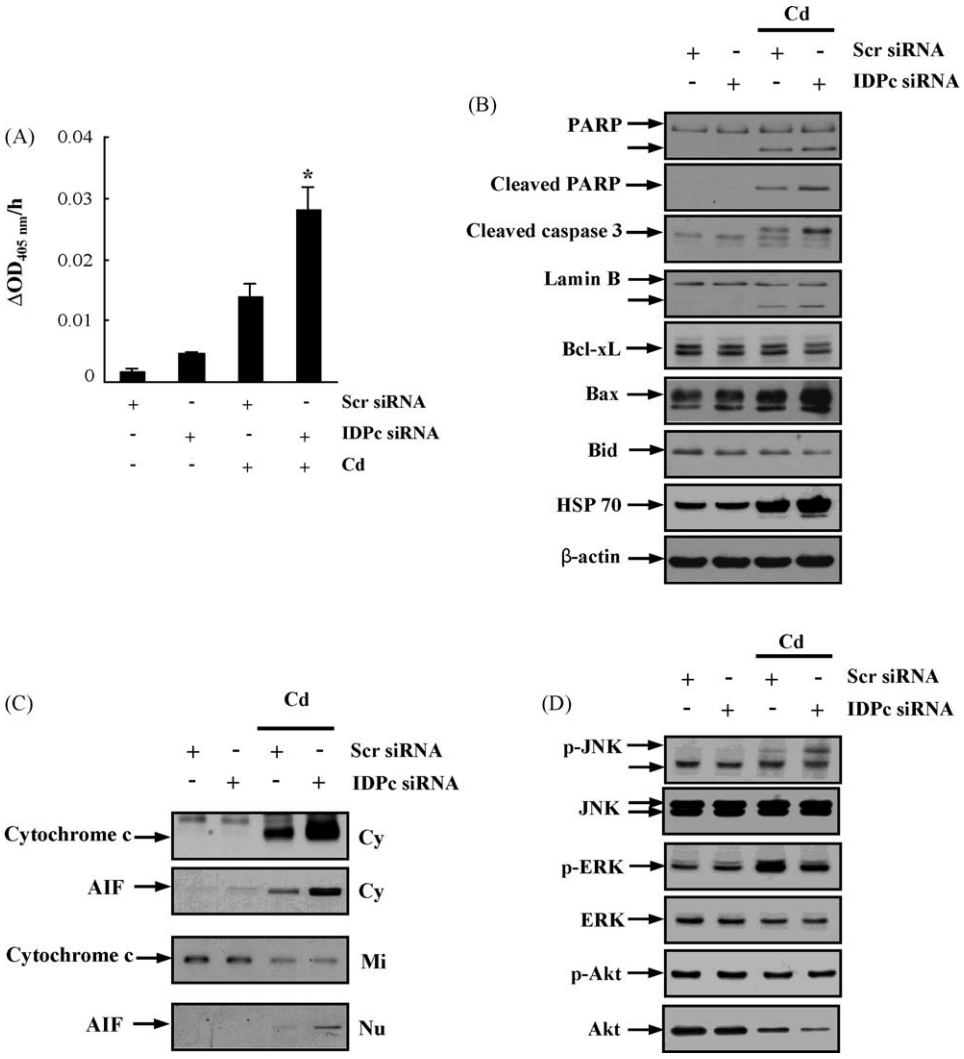

Fig. 4. Modulation of apoptotic marker proteins in IDPc siRNA transfectant HEK293 cells exposed to cadmium. (A) Activation of caspase-3 in HEK293 transfectant cells unexposed or exposed to cadmium. HEK293 cells were lysed and centrifuged, the supernatant was then added to Ac-DEVD-*p*NA and subjected to caspase colorimetric activity. Protease activity of caspase-3 was calculated by monitoring the absorbance at 405 nm. Data are presented as means ± S.D. of three separate experiments. $^{*}p < 0.01$ versus scrambled siRNA-transfected cells exposed to cadmium. (B) Immunoblot analysis of apoptotic marker proteins in HEK293 transfectant cells exposed to cadmium. Cell extracts were subjected to 10–12.5% SDS-PAGE and immunoblotted with antibodies against cleaved caspase-3, PARP, cleaved PARP, lamin B, Bcl-X_L, Bax, Bid and HSP70. β-Actin was used as an internal control. (C) Immunoblot analysis of AIF and cytochrome *c* in cytosolic (Cy), mitochondrial (Mi) and nuclear (Nu) fractions of HEK293 transfectant cells exposed to cadmium. (D) Immunoblot analysis of MAPKs in HEK293 transfectant cells exposed to cadmium. Cell extracts were subjected to 10–12.5% SDS-PAGE and immunoblotted with antibodies against JNK, pJNK, ERK, pERK, Akt and pAkt.

synthetase, the apoptotic susceptibility of IDPc siRNA-transfected HEK293 cells exposed to cadmium was markedly enhanced (Fig. 6A). In contrast, pretreatment with the thiol oxidant NAC suppressed the cadmium-induced increase in DCF fluorescence and the modulation of apoptotic marker proteins in HEK293 cells transfected with IDPc siRNA (Fig. 6B and C). It has been reported that cytosolic Grx (Grx1) plays a vital role in sulfhydryl homeostasis and cell survival [30]. When we examined Grx1 activity in HEK293 cells exposed to cadmium, the inhibition of Grx1 was significantly more pronounced in IDPc siRNA-transfected cells compared with control cells, indicating that IDPc plays a protective role with respect to Grx1 (Fig. 6D). Taken together, these results indicate that decrease in the activity of IDPc, due to the siRNA enhances cadmium-induced apoptosis through the disruption of cellular redox status.

3.5. Role of IDPc siRNA in cadmium-induced mitochondrial damage

ROS are one of the major stimuli that affect mitochondrial integrity and function in apoptosis [31]. We examined the changes in the mitochondrial membrane potential and the MPT using the fluorescent probes JC-1 and rhodamine 123, respectively. Cadmium-induced disruption of the mitochondrial membrane potential and MPT was more pronounced in IDPc siRNA-transfected cells than in control cells (Fig. 7A and B). To determine whether modulation of the mitochondrial integrity was accompanied by changes in mitochondrial ROS, we evaluated the levels of mitochondrial hydrogen peroxide in HEK293 cells using a confocal microscope and the oxidant-sensitive probe DHR 123. As shown in Fig. 7C, the intensity of fluorescence was significantly higher in IDPc siRNA-transfected cells compared to control cells when HEK293 cells were exposed to cadmium.

4. Discussion

Cells have developed an effective and complex mechanism in order to cope with oxidative stress. These cellular defense mechanisms involve antioxidant enzymes, such as SOD, catalase and peroxidases [32]. In addition to using antioxidant enzymes to sequester ROS, low-mass-antioxidants play an essential role, both

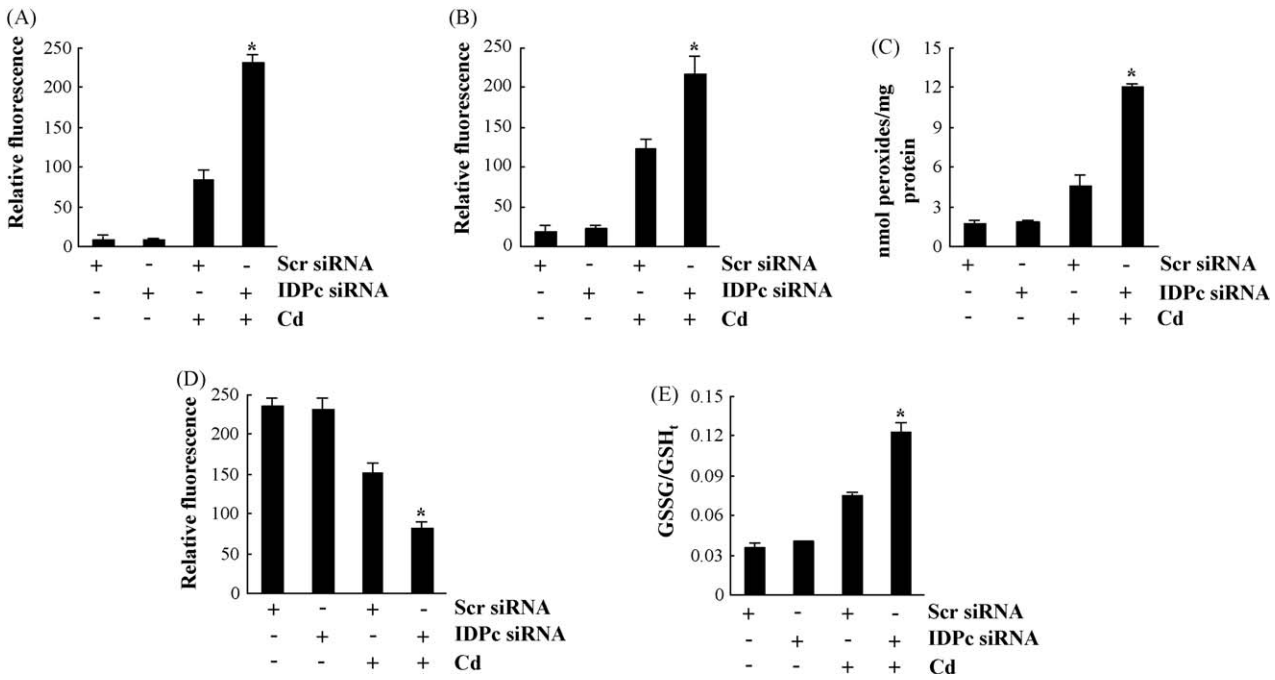

Fig. 5. Cellular redox status of IDPc siRNA transfectant HEK293 cells exposed to 20 μM cadmium for 8 h. (A) Measurement of *in vivo* molecular oxidation. DCF fluorescence was measured in HEK293 transfectant cells exposed to cadmium by fluorescence microscope. (B) Fluorescence image of DHE loaded cells was obtained under laser confocal microscopy. (C) Production of peroxides in HEK293 cells was determined by the method described under Materials and methods. Data are presented as means ± S.D. of five separate experiments. (D) To determine the total GSH levels fluorescence image of CMAC-loaded cells was obtained under microscopy. (E) Ratio of GSSG versus total GSH pool in IDPc siRNA transfectant cells. Data are presented as means ± S.D. of five separate experiments. (A, B and D) The averages of fluorescence intensity were calculated as described [26]. Data are presented as means ± S.D. of three separate experiments. (A–E) $^*p < 0.01$ versus scrambled siRNA-transfected cells exposed to cadmium.

directly and indirectly, in maintaining the cellular redox status. The reducing equivalent NADPH is required for the essential components of antioxidant systems such as GSH turnover, NADPH-dependent thioredoxin systems and the maintenance of catalase activity [13–15]. Although glucose 6-phosphate dehydrogenase (G6PDH), a key enzyme in the pentose phosphate pathway, has long been regarded as the major enzyme involved in generating cytosolic NADPH, we recently reported that IDPc also helps to supply NADPH in the cytosol [33]. Furthermore, it has been shown that IDPc of rat liver has an approximately 20-fold higher specific activity than G6PDH [34]. Since antioxidant enzymes normally act in concert, it is likely that the suppression of IDPc activity exacerbates the ROS-mediated cellular responses. Recently, we reported that IDPm, the mitochondrial counterpart of IDPc, is inactivated by cadmium and that the down-regulation of IDPm expression by an antisense cDNA enhanced cadmium-induced apoptosis [35].

In the present study, we demonstrate that cadmium can inhibit IDPc activity both as a purified enzyme and in cultured cells. In contrast, it has been shown that low concentrations of Cd^{2+} increase the expression of G6PDH [36]. Furthermore, it has been demonstrated that G6PDH activity in ovarian extracts was not diminished in response to treatment with 1 mM Cd^{2+} [37]. The major mechanism by which cadmium suppresses IDPc activity appears to be the direct action of cadmium on IDPc itself. In addition, it is possible that cadmium could inhibit IDPc activity via the generation of free radicals. As Cd^{2+} is not a redox-active metal, it has been proposed that it may induce ROS generation indirectly by inducing the release of redox-active metals such as Cu^{2+} and Fe^{2+} from proteins [38]. The *in vitro* inhibition of cadmium by IDPc was protected by reducing agents such as DTT and GSH. These findings strongly suggest that a thiol redox mechanism may be involved in the inhibitory effect of cadmium on IDPc. It has been shown previously that cadmium oxidizes sulfhydryl groups present in proteins [7]. Thus, it is possible that cadmium could inhibit IDPc activity by interacting with redox-active cysteine residue(s) on the enzyme. The importance of sulfhydryl groups for IDPc activity was confirmed by previous data, which demonstrated that thiol-modifying agents, such as ROS, reactive nitrogen species and lipid peroxidation products, abolished IDPc activity *in vitro* [16,39–41]. Since the addition of the substrate isocitrate-Mg^{2+} prevented the inactivation of IDPc, we conclude that cadmium binding sites are likely to include a cysteine residue near the isocitrate-Mg^{2+} binding site. Site-directed mutagenesis results revealed that Cys^{269}, a residue that presumably resides in the isocitrate-Mg^{2+} binding site, is a target for cadmium.

Our results show that transfecting HEK293 cells with IDPc siRNA sensitized the cells to cadmium-induced apoptosis. Apoptosis was characterized by chromatin condensation, DNA fragmentation, the modulation of mitochondrial integrity and the modulation of apoptotic marker proteins. Since cadmium may trigger cell death by caspase-dependent and/or-independent mechanisms, depending on cell type [42], we investigated the role of caspase-3 in cadmium-induced apoptosis. Our results show that cadmium significantly increased the proteolytic cleavage of procaspase-3 and PARP in IDPc siRNA-transfected HEK293 cells. Pretreatment of cells with the antioxidant NAC almost completely blocked the increase in cleaved caspase-3 and PARP, induced by cadmium in IDPc siRNA-transfected HEK293 cells. This result suggested that the enhancement of ROS generation in cells exposed to cadmium is associated with the activation of the caspase-3 signaling pathway, which contributes to cell death. Bid, a BH3 domain-containing proapoptotic Bcl-2 family member, can be cleaved by caspase-8. The Bid carboxyl-terminal fragment, resulting from this cleavage event, translocates to the mitochondria to induce the release of cytochrome *c*, which is 500 times more numerous than Bax [43]. In the present study, the significant decrease in the proform of the Bid protein indicates that Bid

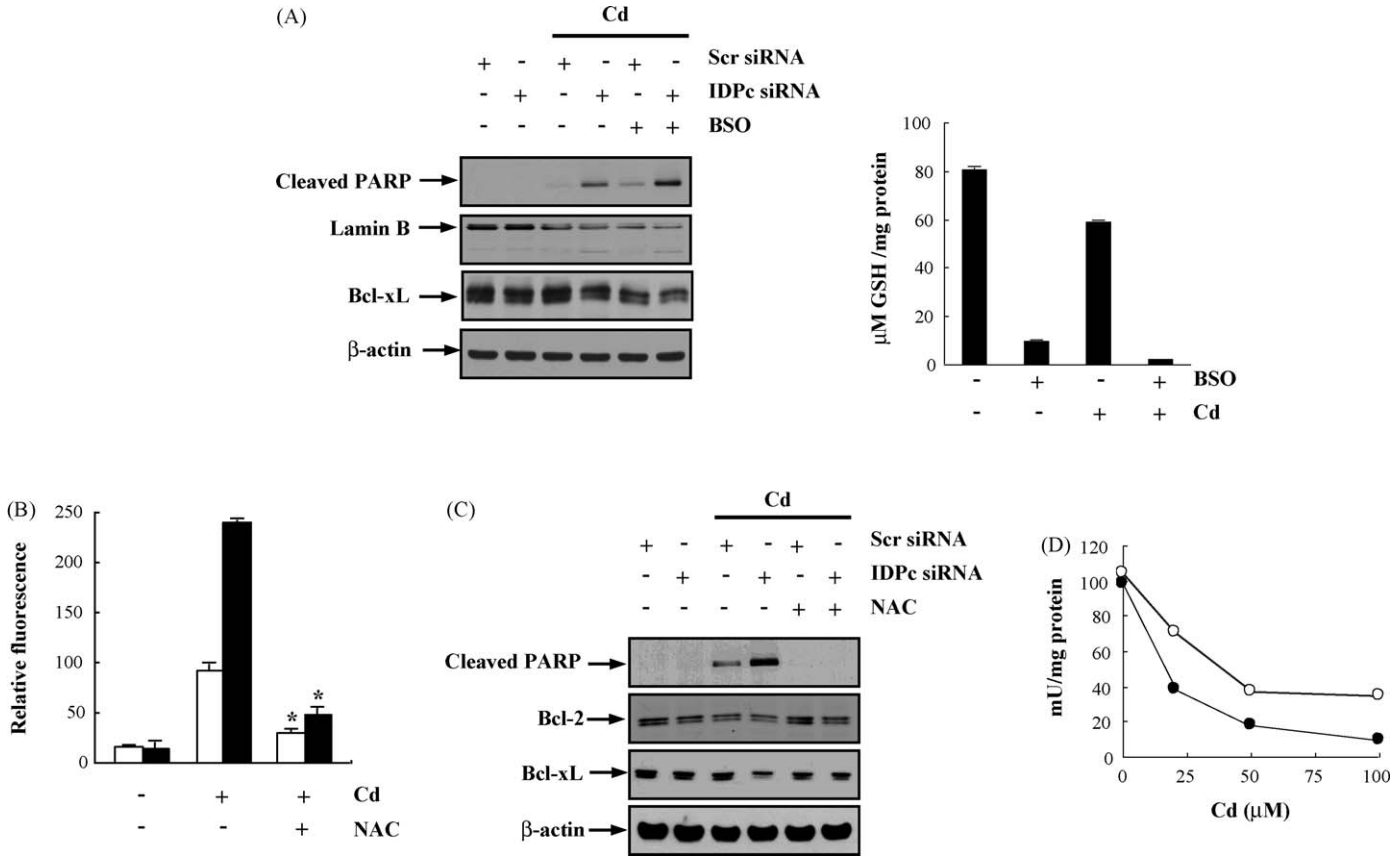

Fig. 6. ROS-mediated mechanism of cadmium-induced apoptosis in HEK293 transfectant cells exposed to cadmium. (A) HEK293 transfectant cells were pre-treated with 1 mM BSO for 12 h, and then cells were exposed to 20 μM cadmium for 8 h. Modulation of apoptotic marker proteins was evaluated by imunoblotting analysis (*left*). The cellular levels of GSH in HEK293 cells exposed to cadmium in the absence and presence of BSO were determined (*right*). Data are presented as means ± S.D. of three separate experiments. (B) IDPc siRNA-transfected HEK293 cells pre-incubated for 2 h in the presence or absence of 5 mM NAC were treated with 20 μM cadmium for 8 h. The averages of fluorescence intensity were calculated as described [26]. Data are presented as means ± S.D. of three separate experiments. Open and shaded bars represent HEK293 cells transfected with scrambled siRNA and IDPc siRNA, respectively. $^*p < 0.01$ versus cells exposed to cadmium in the absence of NAC. (C) Immunoblot analysis of apoptotic marker proteins in cadmium-exposed HEK293 transfectant cells in the presence or absence of NAC. (D) Protective effect of IDPc on cadmium-induced Grx1 inactivation. Activities of Grx1 in IDPc siRNA transfectant HEK293 cells exposed to various concentrations of cadmium for 12 h were determined. Data are presented as means of three separate experiments.

cleavage is markedly increased in IDPc siRNA-transfected cells exposed to cadmium. While another Bcl-2 family member, Bax, promotes cytochrome *c* release, Bcl-2 and Bcl-X_L counteract the effect of Bax and inhibit the release of cytochrome *c* [44]. In our study, the reduction of IDPc activity in IDPc siRNA-transfected cells enhanced the cadmium-induced decrease in Bcl-X_L and increase in Bax. In addition, immunoblotting demonstrated that the translocation of AIF into the nucleus, a mitochondrial protein to be involved in caspase-independent pathway, was significantly enhanced in IDPc siRNA-transfected cells exposed to cadmium. Taken together, these results indicate that the suppression of IDPc expression by the siRNA shifts the cellular redox status to a pro-oxidant state and subsequently enhances the apoptotic pathway in HEK293 cells exposed to cadmium.

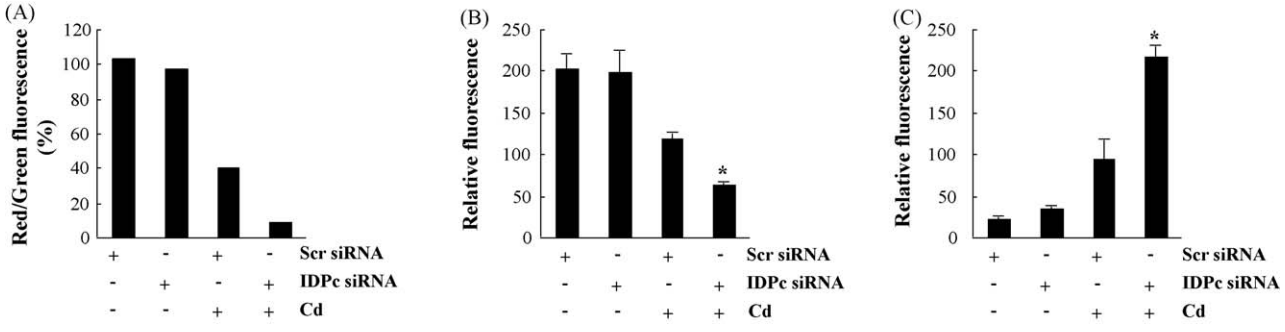

Fig. 7. Mitochondrial function of IDPc siRNA transfectant HEK293 cells exposed to cadmium. (A) HEK293 transfectant cells were incubated with a JC-1 probe for 30 min. Mean (red/green) fluorescence, expressed as a percentage of the control, indicates the ratio of high/low mitochondrial membrane potential. Data are representative of three separate experiments. (B) MPT of HEK293 transfectant cells was measured by the incorporation of rhodamine123 dye into the mitochondria. (C) DHR 123 was employed to detect mitochondrial hydrogen peroxide. DHR 123 fluorescence was visualized by a fluorescence microscope. (A and B) The averages of fluorescence intensity were calculated as described [26]. Data are presented as means ± S.D. of three separate experiments. $^*p < 0.01$ versus scrambled siRNA-transfected cells exposed to cadmium.

Acknowledgments

This work was supported by grants of the Healthcare Technology R&D Project (A084042) and National R&D Program for Cancer Control (0720250), Ministry of Health, Welfare and Family Affairs, Republic of Korea and a Basic Research Program (R01-2008-000-10105-0) from the Korea Science and Engineering Foundation.

References

[1] Lemarié A, Lagadic-Gossmann D, Morzadec C, Allain N, Fardel O, Vernhet L. Hep3B cells: role for calcium in signaling oxidative stress-related impairment of mitochondria and relocation of endonuclease G and apoptosis-inducing factor. Free Radic Biol Med 2004;36:1517–31.
[2] Morselt AF, Leene W, de Groot C, Kipp JB, Evers M, Roelofsen AM, et al. Differences in immunological susceptibility to cadmium toxicity between two rat strains as demonstrated with cell biological methods. Effect of cadmium on DNA synthesis of thymus lymphocytes. Toxicology 1988;48:127–39.
[3] Beyersmann D, Hechtenberg S. Cadmium, gene regulation, and cellular signalling in mammalian cells. Toxicol Appl Pharmacol 1997;144:247–61.
[4] McConkey DJ, Orrenius S. Signal transduction pathways to apoptosis. Trends Cell Biol 1994;4:370–4.
[5] Lyons-Alcantara M, Mooney R, Lyng F, Cottell D, Mothersill C. The effects of cadmium exposure on the cytology and function of primary cultures from rainbow trout. Cell Biochem Funct 1998;16:1–13.
[6] Hultberg B, Andersson A, Isaksson A. Copper ions differ from other thiol reactive metal ions in their effects on the concentration and redox status of thiols in HeLa cell cultures. Toxicology 1997;117:89–97.
[7] Hultberg B, Andersson A, Isaksson A. Alterations of thiol metabolism in human cell lines induced by low amounts of copper, mercury or cadmium ions. Toxicology 1998;126:203–12.
[8] Sun L, Sun TT, Lavker RM. Identification of a cytosolic NADP-dependent isocitrate dehydrogenase that is preferentially expressed in bovine corneal epithelium. J Biol Chem 1999;274:17334–41.
[9] Jennings GT, Stevenson PM. A study of the control of $NADP^+$-dependent isocitrate dehydrogenase activity during gonadotropin-induced development of the rat ovary. Eur J Biochem 1991;198:621–5.
[10] Huh TL, Ryu JH, Huh JW, Sung HC, Oh IU, Song BJ, et al. Cloning of a cDNA encoding bovine mitochondrial NADP(+)-specific isocitrate dehydrogenase and structural comparison with its isoenzymes from different species. Biochem J 1993;292. 705–701.
[11] Oh IU, Inazawa J, Kim YO, Song BJ, Huh TL. Assignment of the human mitochondrial NADP(+)-specific isocitrate dehydrogenase (IDH2) gene to 15q26.1 by in situ hybridization. Genomics 1996;38:104–6.
[12] Plaut GWE, Cook M, Aogaichi T. The subcellular location of isozymes of NADP-isocitrate dehydrogenase in tissues from pig, ox and rat. Biochim Biophys Acta 1983;760:300–8.
[13] Kirsch M, de Groot H. NAD(P)H, a directly operating antioxidant? FASEB J 2001;15:1569–74.
[14] Nakamura H. Thioredoxin and its related molecules: update 2005. Antioxid Redox Signal 2005;7:823–8.
[15] Kirkman HN, Galiano S, Gaetani GF. The function of catalase-bound NADPH. J Biol Chem 1987;262:660–6.
[16] Yang ES, Richter C, Chun JS, Huh TL, Kang SS, Park J-W. Inactivation of $NADP^+$-dependent isocitrate dehydrogenase by nitric oxide. Free Radic Biol Med 2002;33:927–37.
[17] Lee SJ, Yang ES, Kim SY, Kim SY, Shin SW, Park J-W. Regulation of heat shock-induced apoptosis by sensitive to apoptosis gene protein. Free Radic Biol Med 2008;45:167–76.
[18] Luthman M, Holmgren A. Glutaredoxin from calf thymus. Purification to homogeneity. J Biol Chem 1982;257:6686–90.
[19] Zerez CR, Lee SJ, Tanaka KR. Spectrophotometric determination of oxidized and reduced pyridine nucleotides in erythrocytes using a single extraction procedure. Anal Biochem 1987;164:367–73.
[20] Tak JK, Park J-W. The use of ebselen for radioprotection in cultured cells and mice. Free Radic Biol Med 2009;46:1177–85.
[21] Tauskela JS, Hewitt K, Kang LP, Comas T, Gendron T, Hakim A, et al. Evaluation of glutathione-sensitive fluorescent dyes in conical culture. Glia 2001;30:329–41.
[22] Akerboom TPM, Sies H. Assay of glutathione, glutathione disulfide, and glutathione mixed disulfides in biological samples. Methods Enzymol 1981; 77:373–82.
[23] Williams JM, Lea N, Nord JM, Roberts LM, Milford DV, Taylor CM. Comparison of ribosome-inactivating proteins in the induction of apoptosis. Toxicol Lett 1997;91:121–7.
[24] Reers M, Smiley ST, Mottola-hartshorn C, Chen A, Lin M, Chen LB. Mitochondrial membrane potential monitored by JC-1 dye. Methods Enzymol 1995; 260:406–17.
[25] Saikumar P, Dong Z, Patel Y, Hall K, Hopfer U, Weinberg JM, et al. Role of hypoxia-induced Bax translocation and cytochrome *c* release in reoxygenation injury. Oncogene 1998;17:3401–15.
[26] Sundaresan M, Yu ZX, Ferrans CJ, Irani K, Finkel T. Requirement for generation of H_2O_2 for platelet-derived growth factor signal transduction. Science 1995; 270:296–9.
[27] Elbashir SM, Harborth J, Lendeckel W, Yalcin A, Weber K, Tuschl T. Duplexes of 21-nucleotide RNAs mediate RNA interference in cultured mammalian cells. Nature 2001;411:494–8.
[28] Pinot F, Kreps SE, Bachelet M, Hainaut P, Bakonyi M, Polla BS. Cadmium in the environment: sources, mechanisms of biotoxicity, and biomarkers. Rev Environ Health 2000;15:299–323.
[29] Cross TG, Scheel-Toellner D, Henriquez NV, Deacon E, Salmon M, Lord JM. Serine/threonine protein kinases and apoptosis. Exp Cell Res 2000;256:34–41.
[30] Chrestensen CA, Starke DW, Mieyal JJ. Acute cadmium exposure inactivates thioltransferase (Glutaredoxin), inhibits intracellular reduction of protein-glutathionyl-mixed disulfides, and initiates apoptosis. J Biol Chem 2000; 275:26556–65.
[31] Lemasters JJ, Nieminen AL, Qian T, Trost LC, Elmore SP, Nishimura Y, et al. The mitochondrial permeability transition in cell death: a common mechanism in necrosis, apoptosis and autophagy. Biochim Biophys Acta 1998;1366:177–96.
[32] Kil IS, Kim SY, Lee SJ, Park J-W. Small interfering RNA-mediated silencing of mitochondrial $NADP^+$-dependent isocitrate dehydrogenase enhances the sensitivity of HeLa cells toward tumor necrosis factor-α and anticancer drugs. Free Radic Biol Med 2007;43:1197–207.
[33] Lee SM, Koh HJ, Park DC, Song BJ, Huh TL, Park J-W. Cytosolic $NADP^+$-dependent isocitrate dehydrogenase status modulates oxidative damage to cells. Free Radic Biol Med 2002;32:1185–96.
[34] Veech RL, Eggleston LV, Krebs HA. The redox state of free nicotinamide-adenine dinucleotide phosphate in the cytoplasm of rat liver. Biochem J 1969;115:609–19.
[35] Kil IS, Shin SW, Yeo HS, Lee YS, Park J-W. Mitochondrial $NADP^+$-dependent isocitrate dehydrogenase protects cadmium-induced apoptosis. Mol Pharmacol 2006;70:1053–61.
[36] Xu J, Maki D, Stapleton SR. Mediation of cadmium-induced oxidative damage and glucose-6-phosphate dehydrogenase expression through glutathione depletion. J Biochem Mol Toxicol 2003;17:67–75.
[37] Carattino MD, Peralta S, Perez-Coll C, Naab F, Burlon A, Kreiner AJ, et al. Effects of long-term exposure to Cu^{2+} and Cd^{2+} on the pentose phosphate pathway dehydrogenase activities in the ovary of adult Bufo arenarum: possible role as biomarker for Cu^{2+} toxicity. Ecotoxicol Environ Safety 2004;57:311–8.
[38] Stohs SJ, Bagchi D. Oxidative mechanisms in the toxicity of metal ions. Free Radic Biol Med 1995;18:321–36.
[39] Lee JH, Yang ES, Park J-W. Inactivation of $NADP^+$-dependent isocitrate dehydrogenase by peroxynitrite: Implications for cytotoxicity and ethanol-induced liver injury. J Biol Chem 2003;278:51360–71.
[40] Lee SM, Huh TL, Park J-W. Inactivation of $NADP^+$-dependent isocitrate dehydrogenase by reactive oxygen species. Biochimie 2001;83:1057–65.
[41] Yang JH, Yang ES, Park J-W. Inactivation of $NADP^+$-dependent isocitrate dehydrogenase by lipid peroxidation products. Free Radic Res 2004;38: 241–9.
[42] Chen L, Liu L, Huang S. Cadmium activates the mitogen-activated protein kinase (MAPK) pathway via induction of reactive oxygen species and inhibition of protein phosphatases 2A and 5. Free Radic Biol Med 2008;45:1035–44.
[43] Li H, Zhu H, Xu CJ, Yuan J. Cleavage of Bid by caspase 8 mediates the mitochondrial damage in the Fas pathway of apoptosis. Cell 1998;94: 491–501.
[44] Kluck RM, Bossy-Wetzel E, Green DR, Newmeyer DD. The release of cytochrome *c* from mitochondria: a primary site for Bcl-2 regulation of apoptosis. Science 1997;275:1132–6.